Sensors and Actuators B 202 (2014) 1338–1348

Contents lists available at ScienceDirect

Sensors and Actuators B: Chemical

journal homepage: www.elsevier.com/locate/snb

Scanning fluorescence-based ultrasensitive detection of dengue viral DNA on ZnO thin films

M. Adiraj Iyer[a,b], Goldie Oza[a], S. Velumani[a,d,*], Arturo Maldonado[a], Josue Romero[a], M. de L. Muñoz[c], M. Sridharan[b], R. Asomoza[a], Junsin Yi[d]

[a] Sección de Electrónica del Estado Sólido del, Departamento de Ingeniería Eléctrica, CINVESTAV, Mexico City, Mexico D.F.
[b] Centre for Nanotechnology & Advanced Biomaterials, SASTRA University, Thanjavur, India
[c] Genética y Biología Molecular, CINVESTAV, Mexico City, Mexico D.F.
[d] School of Information and Communication Engineering, Sungkyunkwan University, 300 Cheoncheon-Dong, Jangan-Gu, Suwon, Korea

ARTICLE INFO

Article history:
Received 23 September 2013
Received in revised form 1 June 2014
Accepted 2 June 2014
Available online 7 June 2014

Keywords:
Zinc Oxide
Ultrasonic Spray Pyrolysis
Dengue
Fluorescence
Biosensor

ABSTRACT

In this article, ZnO thin film acts as a matrix to bind with a sequence specific probe strand, which is employed as a recognition element and is involved in sensing the complementary DNA of dengue virus specific serotypes. ZnO thin films possess high surface area, high catalytic efficiency with an isoelectric point of ~9.5, thus leading to strong electrostatic attraction and strong adsorption capability towards negatively charged DNA having an isoelectric point of 4. ZnO thin film deposition is carried out by ultrasonic spray pyrolysis (USP) at the temperature of 450 °C using dry air as the carrier gas along with 0.1 M of zinc acetate as the precursor to obtain transparent films with a thickness of around 150–200 nm. X-ray diffraction data show the dominant peak corresponding to (100). The morphology of ZnO thin films was analyzed using field emission-scanning electron microscope (FE-SEM) and atomic force microscope (AFM). The optical characteristics of thin films were studied using UV-spectroscopic analysis, which confirms the band gap of the film to be 3.3 eV. Further, sequence specific DNA immobilization is carried out for the bio-functionalization of ZnO thin films to detect 4 DENV serotypes, thus enabling simultaneous detection in an array having sensitivity in the range of 1×10^{-15} moles of DNA.

1. Introduction

Dengue virus belongs to the Flaviviridae family comprising of 4 unique serotypes (DEN-1, DEN-2, DEN-3 and DEN-4) and consists of an antigenic complex in the genus *Flavivirus*. This disease is transmitted by a diurnal mosquito, *Aedes aegypti*, which feeds on human blood [1]. This mysterious virus after infection induces life-long immunity towards the same serotype, but renders significantly less protection against infection from other serotypes [1]. Clinical manifestations as a consequence of dengue infections can be asymptomatic initially but later can lead to severe diseases such as dengue haemorrhagic fever (DHF)/dengue shock syndrome (DSS) and eventually death [2].

Clinical symptoms of dengue fever (DF) include myalgia, arthralgia, maculopapular rash, petechiae, bruising or thrombocytopenia. This can transform into severe DHF/DSS, which is manifested by plasma extravasation, high fever, bleeding, thrombocytopenia and haemoconcentration. Due to the non-availability of anti-viral therapeutics, patients can be treated by fluid management and electrolyte administration. This is possible only with efficient diagnosis of the virus as well as identification of the serotype.

Many diagnostic tests can be used and are classified as either direct or indirect. The direct diagnostic method involves the type-specific determination of the virus during acute infection. This constitutes live virus isolation or detection of various components such as RNA or antigen in serum, plasma, whole blood and infected tissues within 3–5 days of manifestation of symptoms [2]. The indirect test involves detection of IgM antibodies within 5 days after the onset of symptoms during primary as well as secondary infections, and detection of IgG antibodies after 10–15 days of clinical manifestation. Many serological assays can be used, such as the IgM capture enzyme-linked immunosorbent assay (MAC-ELISA) [3], haemagglutination inhibition assays (HAE) [4], immunofluorescence assays [5–7] and the plaque reduction neutralization test (PRNT) [8]. All

* Corresponding author at: Sección de Electrónica del Estado Sólido, Departamento de Ingeniería Eléctrica, CINVESTAV-IPN, Av. Instituto Politecnico Nacional 2508, San Pedro Zacatenco, Gustavo A. Madero, 07360 Ciudad de México, Distrito Federal, Tel.: +5255-5747-3800.
E-mail address: velu@cinvestav.mx (S. Velumani).

http://dx.doi.org/10.1016/j.snb.2014.06.005
0925-4005/

of the above tests are problematic as they exhibit broad cross-reactivity with other flaviviruses. Some also exhibit non-specific reaction with patients suffering from malaria and leptospirosis. To circumvent the problems of sensitivity and specificity, molecular assays based on nucleic acid amplification by reverse transcriptase (RT)-PCR, nucleic acid sequence-based amplification (NASBA) real-time PCR and reverse transcription–loop-mediated isothermal amplification (RT-LAMP) assay are assumed to rapidly detect and differentiate dengue virus serotypes [2]. Recently, we have described and tested a microarray-based method for the screening of dengue virus serotypes using RT-PCR amplification.

However, the present study describes the development of a fluorescence-based method for rapid, inexpensive, field-compatible and ultrasensitive dengue serotype cDNA detection without any need for amplification. The fluorophore-labelled DEN serotype probe sequence can selectively bind to a serotype specific dengue DNA target sequence on a fluorescence enhancing apparatus. To enhance the fluorescence detection capacity, two important aspects of biomolecular detection have been taken into account:

1) designing of a good quality fluorophore and
2) developing an enhanced detection paraphernalia.

Many organic, inorganic and hybrid labels can be used as substrates for the prevention of photobleaching of fluorescent dyes or fluorophores. Such labels help in the measurement of different fluorophores using a single excitation source [9–11]. The exploration of metallized substrates for enhanced quantum yield and photostability of fluorophores has facilitated an interest in the development of ZnO nanoplatforms.

ZnO thin films have attracted considerable attention due to their broad range of electrical, optical and mechanical properties. ZnO possesses a direct band gap of 3.2–3.4 eV at 300 K, good chemical stability, distinct electrical and optoelectronic properties and has a large exciton binding energy (60 meV), thus causing lasing action considerably above room temperature [12–14]. The tunable band gap and high transparency of ZnO have made it a promising candidate for short-wavelength and transparent optoelectronic devices such as light-emitting diodes (LEDs) [15], solar cells [16], sensors [17], field effect transistors [18] lasers [19] and field-emitters [20]. Moreover, the ZnO nanostructure is advantageous as an efficient nanoplatform due to its high specific surface area, non-toxicity, chemical stability and electrochemical activity.

Biomacromolecules such as DNA and enzymes can be immobilized on an electroactive ZnO nanoparticle for detection of target oligonucleotide or metabolite. Liu et al. have designed a DNA microarray using ZnO/Au nanocomposites bio-functionalized with thiol-oligonucleotide probes for detection of a target sequence of oligonucleotide as low as 1 fM, with an aid of resonant multiple phonon Raman signal [21]. A ZnO nanotube array was prepared for use as a working electrode for the fabrication of an enzyme-based glucose biosensor through immobilization of glucose oxidase in combination with a Nafion coating. Such a biosensor has a lower limit of detection (LOD) for glucose at 10 μM [22]. Zhu et al. demonstrated that semiconducting ZnO can mediate direct electron transfer reactions of microperoxidase, causing an enhancement of its electrocatalytic activity for effective reduction of hydrogen peroxide for the construction of a biosensor [23]. Umar et al. developed a highly sensitive ZnO-based cholesterol amperometric biosensor. They used a detection limit of 0.37 nM, and very low values of Michaelis Menten constant (i.e., 4.7 mM) indicated very high affinity of ChOx [24]. The high isoelectric point of ZnO nanoparticles facilitated adsorption of a low isoelectric point tyrosinase, thus developing a mediator-free phenol biosensor [25].

In this article, engineered nanoscale ZnO nanostructures act as an efficient platform for enhancing fluorescence detection capacity towards sensing cDNA without the need for amplification. Such inexpensive and rapidly synthesized ZnO platform developed by "ultrasonic spray pyrolysis" (USP) are used for the first time in enhanced fluorescence detection of all the 4 serotypes of dengue virus labelled with 4 different fluorophores in one single detection system. Such ZnO platforms are characterized by XRD, FE-SEM, AFM and UV-spectroscopy for the comprehension of structural and optical properties. ZnO possesses high isoelectric point (IEP) of about 9.5 and is capable of interacting with a low IEP DNA having a value of ~4. The proficient electroactive surface provided by ZnO thin films can be used for biosensor development since it is chemically inert, non-toxic, biocompatible and possesses enhanced charge transfer capability. Our results demonstrate that we can efficiently fabricate ZnO thin films as a fluorescence enhancer that can be assembled into a tailor-made array. This array can simultaneously perform qualitative as well as quantitative detection of 4 serotypes of dengue virus on the same platform, thus endorsing high throughput and sensitive, multiplexed fluorescence detection of DNA. The sensor surface prepared in this way has a reversible nature, thus enhancing its reusability.

2. Experimental details

2.1. ZnO thin film

ZnO thin films were deposited onto thoroughly cleaned glass substrates (Corning optical microscope slides) of size 2.5 cm × 5 cm. (The substrates were cleaned by ultrasonication in surfactant, deionized water and ethanol in sequence and dried under flow of compressed air.) Precursor solution was prepared by dissolving zinc acetate ($ZnAc_2$) at a concentration of 0.1 M in deionized water. Acetic acid was added drop-wise to avoid precipitation of zinc hydroxide. The precursor was then loaded in the deposition system that constitutes a piezoelectric transducer operating at a frequency of 1.2 MHz [Ultrasonic Humidifier HUM 006, Sunshine Co., Mexico] and sprayed onto the cleaned glass substrates. The droplets of precursor solution were produced using an ultrasonic generator. These droplets were then navigated towards the substrate by dry air (carrier gas) in the form of a jet. The substrates were placed on a melted tin bath and the temperature was measured below the substrate using a thin chromel–alumel thermocouple jacketed by stainless steel. The temperature of the hot plate was maintained at 450 °C with an error of 1 °C [26]. The formation of ZnO occurred as per the following equation:

$$Zn(CH_3COO)_{2(aq.)} \xrightarrow[\Delta]{} ZnO + 2CH_3COOH \quad (1)$$

The substrates were coated for 2, 5, 7 and 10 min at a mist flow rate of 3 mL/min while the carrier gas was maintained at 2 L/min. While all parameters such as substrate temperature and carrier gas flow rate have already been optimized in previous reports [27,28], immobilization of DNA is dependent on thickness of the film for proper adsorption and enhanced fluorescence activity, resulting in the need to determine optimum deposition time. The films deposited in this way were characterized using X-ray diffraction (XRD), field emission scanning electron microscopy (FE-SEM), UV–visible spectroscopy, atomic force microscopy (AFM) while the thickness of the film was determined by cross-sectional FE-SEM.

2.2. DNA immobilization

The coated substrates (films) were then immobilized with DNA. Fluorescent dye labelled probe [*P*] strands derived from 4 different serotypes of dengue virus were procured from The Midland Certified Reagent Company (Midland, TX, USA) and used after diluting to 1 nM concentration. The 4 probe strands as mentioned in

Table 1
Chemical composition of ZnO thin films as per energy dispersive analysis of X-ray.

Element	Series	unn. C [wt.%]	norm. C [wt.%]	Atom. C [at.%]	Error (1 sigma) [wt.%]
Oxygen	K-series	29.53	23.76	56.02	3.69
Zinc	L-series	94.74	76.24	43.98	5.82
Total		124.27	100.00	100.00	

Table 1 were then used for immobilization on ZnO thin films. One microlitre of 1 nM DNA solution was immobilized on thin films at an incubation temperature of 42 °C using a humidity chamber in a hybridization oven.

2.3. Hybridization detection

A target [*T*] analyte strand with a detection volume of 1 μL at a concentration of 1 nM was used for hybridization with corresponding probe [*P*] strand immobilized on ZnO. The target [*T*] strands were allowed to hybridize in the hybridization oven at 42 °C for 2 h. The films were then washed repeatedly with SDS, deionized water and ethanol. One ZnO thin film substrate was left in the water for a prolonged period (24 h) for reproducibility studies. Subsequently, laser induced fluorescence scanner was used to observe fluorescence on the film. *T* and *P* strands were spotted sequentially as a 4 × 4 array using T_i and P_i (i = 1, 2, 3, 4), respectively, with 1, 2, 3, 4 corresponding to the serotypes.

3. Results and discussions

3.1. ZnO thin film

3.1.1. Mechanism of thin film growth

A plausible reaction mechanism for films deposited using USP has been reported by Paraguay et al. [29]. Such as-deposited ZnO thin films exhibit good surface uniformity, high optical transmittance and *c*-axis orientation. The strongly adhered ZnO film is the effect of the deposition of aerosol droplets onto the heated glass substrate due to the pyrolytic process. The following steps explain the whole process of deposition:

1) Basic zinc acetate is sublimed to a gaseous complex, releasing water vapour as a by-product, thus reducing the amount of residual carbon in the film. This helps in the final decomposition reaction due to the hydrolysis of the basic zinc acetate.
2) The entire gaseous complex is then adsorbed near the heated glass substrate and undergoes decarboxylation, thus releasing acetone.
3) Ultrasonic spray pyrolysis of basic zinc acetate following mist formation is finally deposited at the substrate temperature of 450 °C and the deposition rate is mass transport controlled. This indicates that the deposition rate is a non-conventional convective mass transport process since the kinetics of the entire reaction is enhanced to such an extent that it is totally controlled by mass transfer reaction [30].

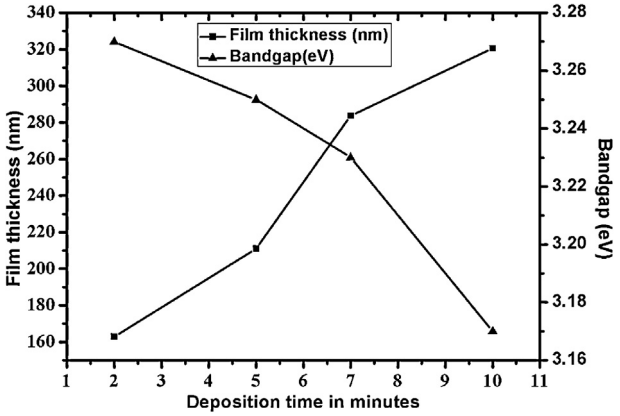

Fig. 2. Variation in film thickness and band gap at different deposition times.

3.1.2. Optical properties

ZnO thin film deposition occurred as a result of the pyrolytic process taking place when droplets were sprayed on heated glass substrates. Fig. 1 shows the percentage transmittance versus wavelength for thin films prepared at different deposition times (2, 5, 7 and 10 min). A sharp cut off occurred near 370 nm in the transmission spectra and an increment was found to be remarkably sharp in the region of 370–400 nm. The value of transmittance in the visible region increases with an increase in the deposition time, up to 5 min and then decreases as deposition time further increases. This indicates that films deposited for 5 min have fewer defects, smaller size and better crystallinity. As deposition time increases, in spite of better crystallinity, the size increases as can be verified

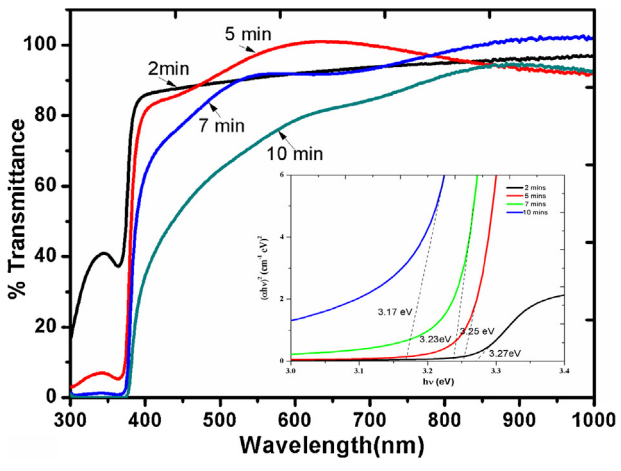

Fig. 1. Transmittance of ZnO thin films deposited for 2, 5, 7 and 10 min and inset shows band gap of ZnO thin films at different deposition times.

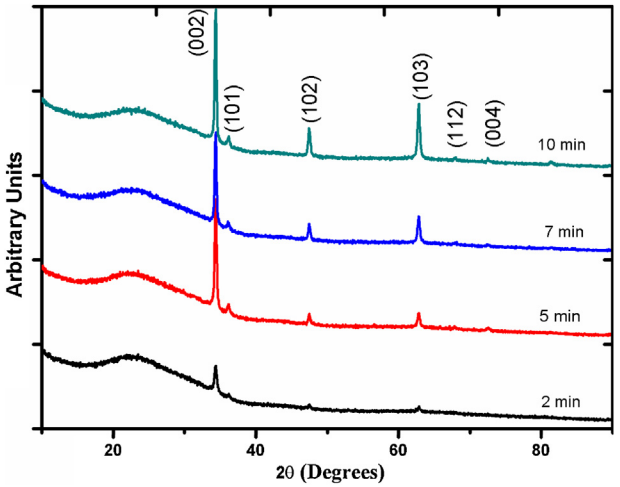

Fig. 3. XRD of ZnO thin film at different deposition times of 2, 5, 7 and 10 min.

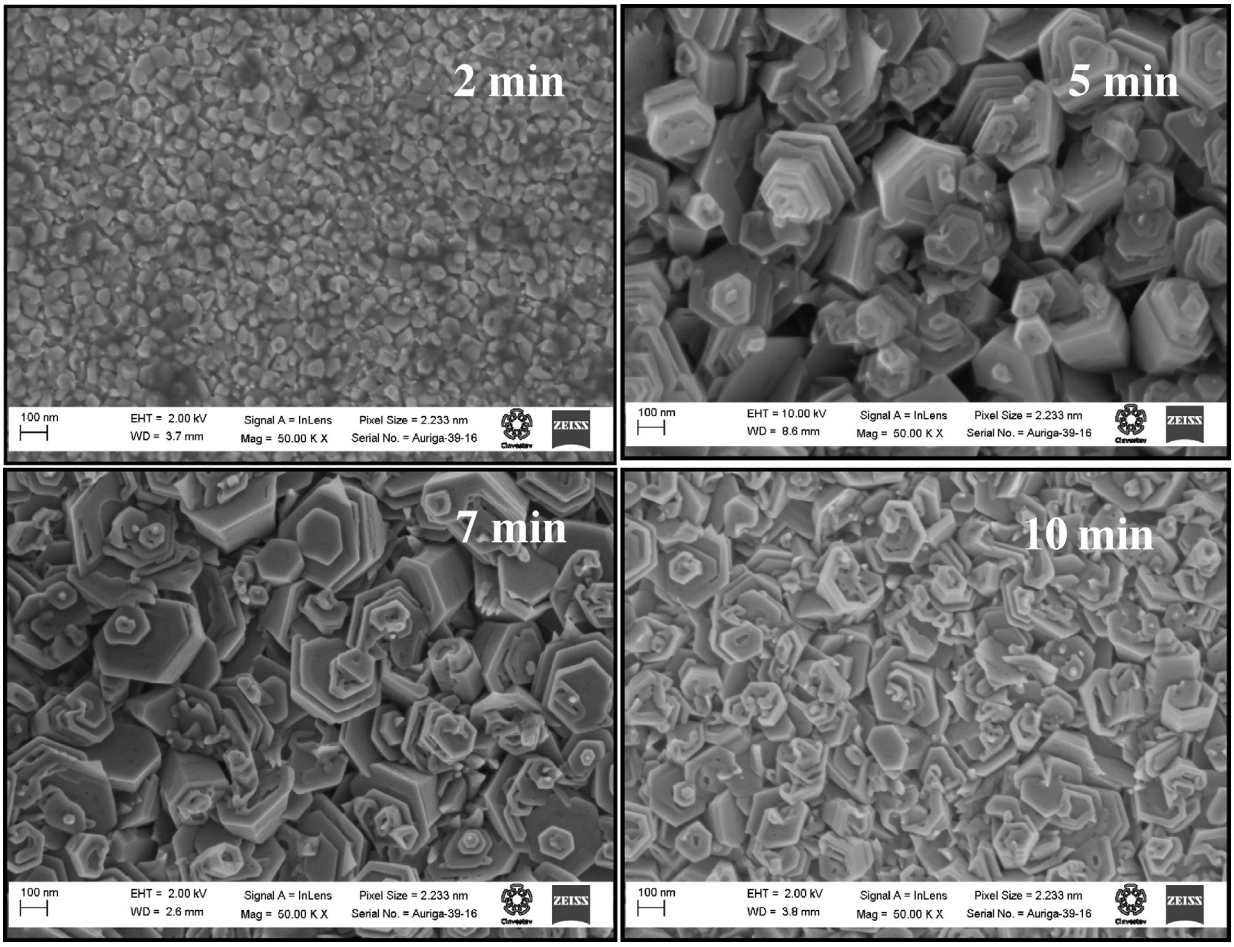

Fig. 4. Scanning electron micrographs of ZnO thin films deposited at different deposition times of 2, 5, 7 and 10 min.

with XRD and FE-SEM analysis (Figs. 3 and 4). The average percentage of transmittance in the spectral range of 400–1000 nm was decreasing from 97% to 70% with an increase in the deposition time from 2 to 10 min. This decrement is due to increased thickness of the film, thus leading to the formation of a large number of absorbing species [31]. While the films are sharply transparent at lower energies, even in the transparent regime, some transmitted intensity is lost due to scattering of light from the grain boundaries, with increase in scattering as grain size decreases [32]. This affects the fluorescent detection of dengue serotypes since this study focuses on the interplay between scattering (electromagnetic effects) and fluorescence (molecular dynamics).

The inset of Fig. 1 shows the optical energy band gap of ZnO thin film estimated from absorption measurement in the wavelength range of 400–750 nm. The absorption coefficient (α) and photon energy ($h\nu$) gives a calculation of the optical band gap energy which can be estimated using the following relationship [33,34]

$$\alpha = \frac{A(h\nu - E_g)^{1/2}}{h\nu} \quad (2)$$

where α is the absorption coefficient, A is the proportionality constant and $h\nu$ is the photon energy, ν is frequency and E_g is the band gap. The band gap for the deposited thin films can be measured by plotting $(\alpha h\nu)^2$ as a function of $h\nu$, and extrapolating $(\alpha h\nu)^2$ to the energy $h\nu$, where $(\alpha h\nu)^2$ corresponds to zero. The band gap values red-shifts from 3.27 to 3.17 eV, as the film thickness increases from 163 to 325.59 nm with increasing deposition time, as can be seen in Fig. 2. These shifts may be due to various factors such as grain size, structural parameters and lattice strain, carrier concentration, or deviation from stoichiometry. These shifts in the band gap energy could also be related to quantum confinement, which is clearly dependent on crystallite size. In this case, the sizes are very large compared to the ZnO exciton Bohr radius, in the order of 250–380 Å calculated from Scherrer formula at different deposition times (2–10 min). The shift in the band gap may also be due to the out-of-plane strain in the crystallites [35].

3.1.3. Structural properties

X-ray diffraction pattern of the as-deposited films at different deposition times (2–10 min) is shown in Fig. 3. The diffraction peaks that correspond to the (002), (101), (102), (103), (112) and (004) planes were determined for hexagonal (wurtzite) ZnO thin films. The (002) peak was found to increase with an increase in the deposition time, with all the remaining constant. This increase in the preferred orientation towards the c-axis or the (002) plane may be due to the atoms possessing enough diffusion activation energy, thus occupying an exact site in the crystal lattice, with the grains becoming increasingly crystalline as deposition time increases. The average crystallite size t corresponding to the (002) plane can be estimated by the Scherrer formula [36]

$$t = \frac{0.9\lambda}{B\cos\theta} \quad (3)$$

where λ is the X-ray wavelength corresponding to 0.154 nm, θ is the Bragg diffraction angle and B is the full width at half maximum (FWHM). The FWHM of this most dominant (002) plane decreases as deposition time increases from 2 to 10 min, as can be seen in Table 2, thus leading to the enhancement of crystallinity caused

Table 2
Average crystallite size and grain size of ZnO as per XRD and FE-SEM, respectively, along with their FWHM values for different deposition time.

Deposition time(min)	FWHM in degrees	2θ	Crystallite size (nm) as per XRD	Average grain size (nm) as per FE-SEM
2	0.3460	34.6	25.39	42
5	0.3121	34.6	30.8	72.77
7	0.2865	34.6	38	99.07
10	0.2816	34.6	38.2	117.76

by the supply of sufficient thermal energy for longer duration. The average crystallite size of ZnO increases with an increase in the deposition time from 2 min (25.39 nm) to 10 min (38.2 nm). As the deposition time increases, the crystallite size tends to increase due to the mass transfer of Zn and O atoms in (002) orientation which is confirmed by XRD analysis in Fig. 3.

3.1.4. Surface morphology and film thickness

FE-SEM and AFM analysis of ultrasonic spray-deposited films was performed to comprehend surface morphology, thickness and roughness of films. The surface roughness, uniformity and compactness of the films can be clearly seen from Fig. 4. The FE-SEM micrographs show an increase in the average grain size of hexagonal (wurtzite) ZnO thin films as deposition time increases from 2 min (24.26 nm) to 5 min (158.77 nm), but the average size remains the same as deposition time increases to 10 min (162.7 nm). Moreover, the films are found to be compact and uniform at 2 min, but as the deposition time increases, more defects are introduced in the grain, exhibiting coiled growth of the hexagonal structures in a particular plane, causing more roughness in the films. This provides a greater active area for the attachment of DNA strands during detection. The large discrepancy in the average grain sizes obtained from SEM and XRD is due to the mean dimension of the crystallites, which is perpendicular to the diffraction plane using XRD and aggregation, as seen in the SEM images in Fig. 4. The grains observed in the SEM images in Fig. 4 are clearly observed to be agglomerates of smaller crystallites causing an increase in the grain size. Energy dispersive analysis of X-rays shows the formation of ZnO with nearly 50% and 50% atomic composition of Zn and O, respectively, as demonstrated in Fig. 5**.** A slight excess of oxygen content is observed, which may be attributed to the adsorption of ambient gases onto the film. Cross-sectional FE-SEM as seen in Fig. 6 depicts the thickness of ZnO thin films, which is found to increase as deposition time increases.

Atomic force micrographs over an etched edge were imaged in tapping mode using a silicon nitride tip in order to measure the thickness of the film and to determine the topography of the surface. As shown in Fig. 7, the film shows a thickness of about 38–124 nm as deposition time increases from 2 to 10 min. The topographical image shows the surface to be rough with a significant pore formation more clearly seen in the FE-SEM images. The three-dimensional image shows the rough character of films

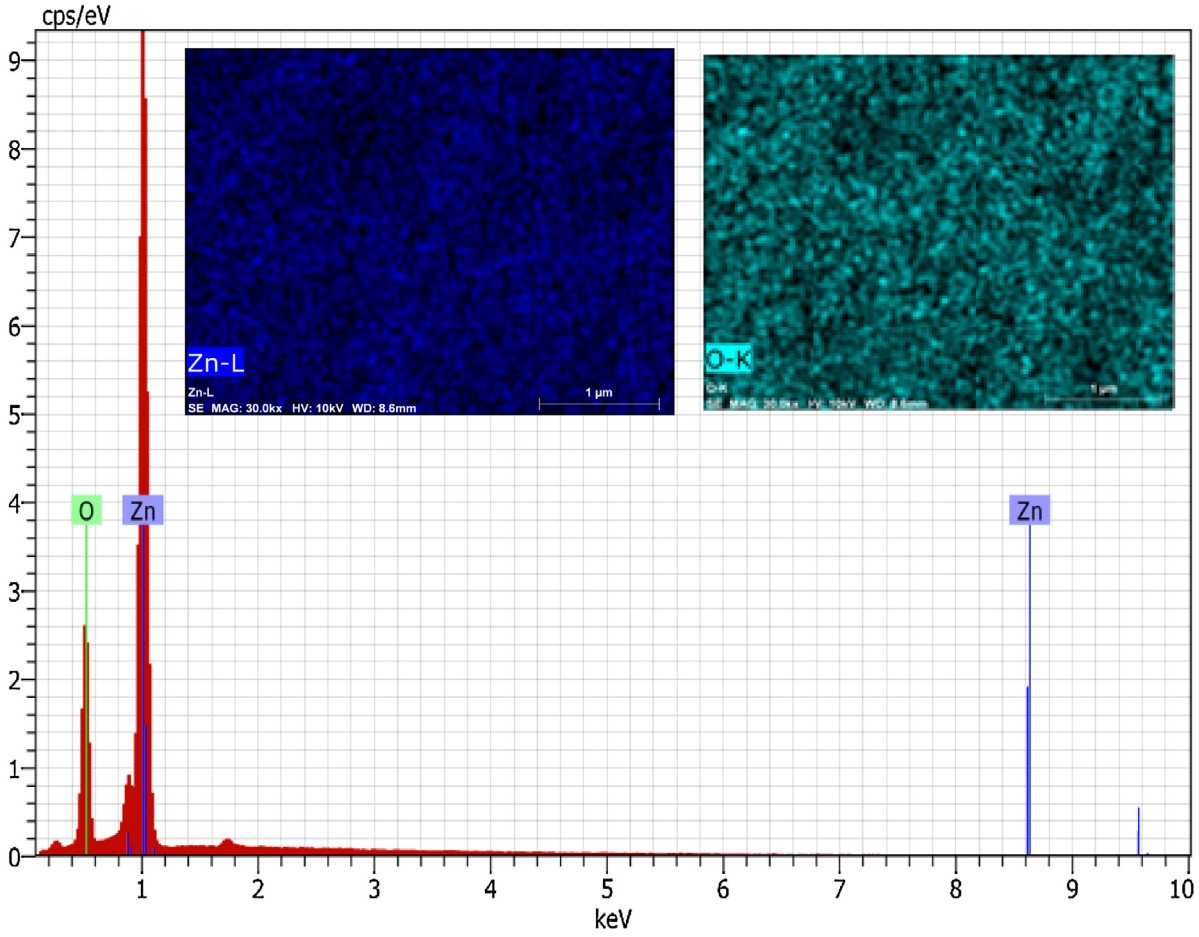

Fig. 5. Representative EDS of ZnO thin film.

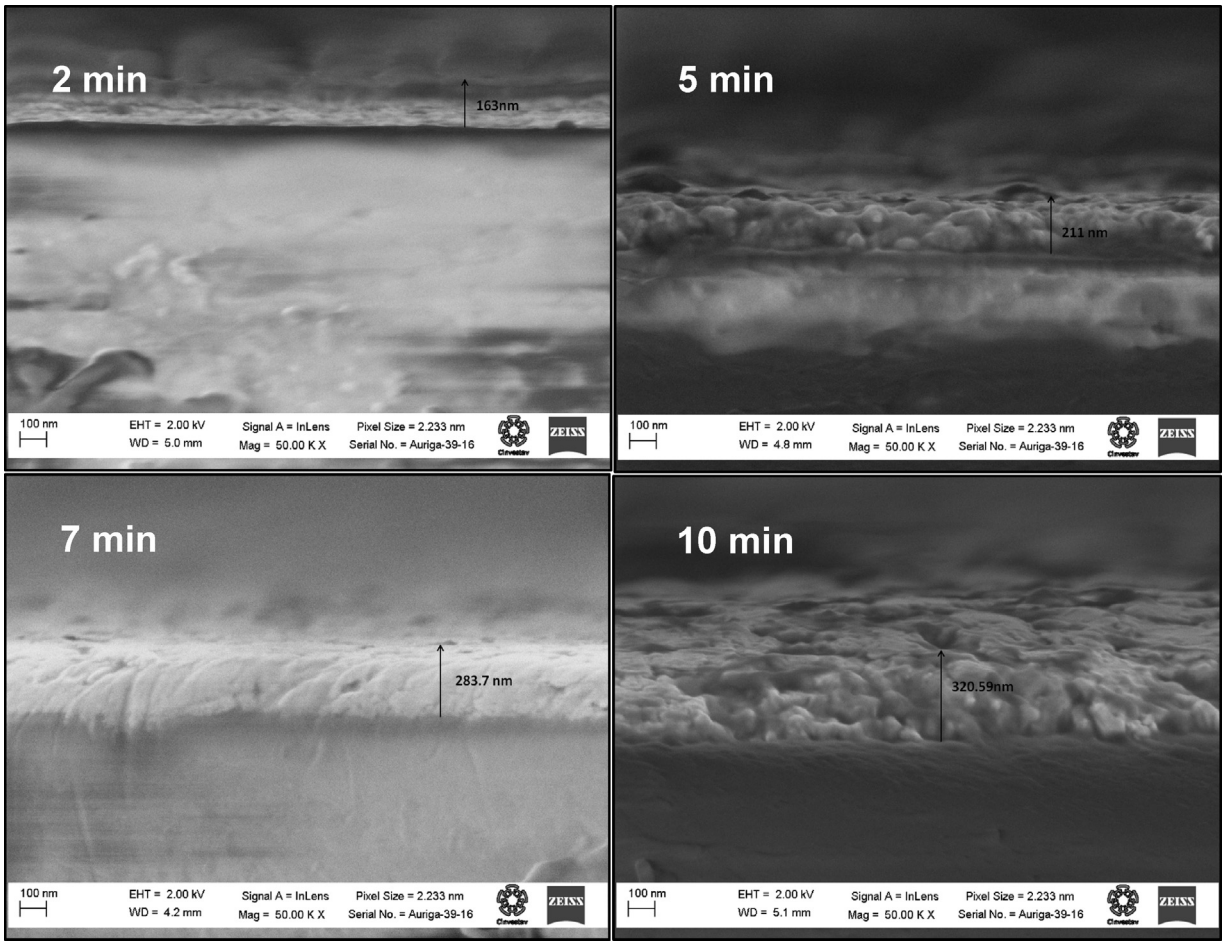

Fig. 6. Cross-sectional scanning electron micrographs of ZnO thin films for thickness at different deposition times of 2, 5, 7 and 10 min.

over the scanned area. AFM also shows the grain agglomeration along with the formation of tall columnar structures approximately 38–124 nm in height distributed across the surface, which enhances the roughness and surface area of the film. From the SEM and AFM images, we can say that the surface area is enhanced to present a more electroactive area for the electrostatic immobilization of the *P* and *T* strands of DNA.

3.2. DNA immobilization

The most proficient ZnO thin film as determined from AFM, SEM and XRD is found to be at a deposition time of 5 min. This is because, there is no further increase in the average crystallite size and average grain size of the particles as deposition time increases. Moreover, while the crystallinity remains the same, the porosity starts to decrease as deposition time increases. A deposition time of 5 min is found to be the most significant for DNA immobilization, since both crystallinity and porosity are at equilibrium. Many popular chemical methods of DNA immobilization have been used for the fabrication of sensors, making immobilization by electrostatic attraction. The zeta potential measurement of ZnO thin film [37] has shown that ZnO is a favourable material for the immobilization of DNA on its surface due to the presence of a positive charge on its surface at pH 7–8. Transparent nanostructured metal oxides display unique capability for promoting enhanced electron transfer kinetics between the electrodes and sensing element. The metal oxide nanoparticles that is considered to be most efficient is the ZnO nanoparticles, which has achieved technological importance for the development of biosensors and dye-sensitized solar cells since they tend to possess high surface area, catalytic efficiency and higher isoelectric point (i.e., ~9.5). This consequently allows strong electrostatic immobilization of negatively charged DNA (isoelectric point at 4) on ZnO nanoparticles [38]. This means that ZnO surface is positively charged when DNA is immobilized. Electrostatic attraction occurs between the positively charged ZnO surface and the negatively charged DNA due to its numerous negative charges from the phosphodiester backbone. The charge density of DNA is relatively high due to the oxygen atoms at every level. Hence, DNA contains one fundamental negative charge per base pair (e/bp). The sequences used in this experiment are an average of 215–250 bp long. This implies a large negative charge and hence stronger forces of electrostatic attraction. This force can be given by Coulomb's law as:

$$F = \frac{-1}{4\pi\varepsilon_0} \cdot \frac{q_2}{r^2} \tag{4}$$

In this case, a higher number of base pairs implies that the molecule will also have a higher number of charges, making the Coulombic forces stronger, resulting in a stronger attraction. Also, the positively charged ZnO and negatively charged DNA interact in the presence of a medium such as water. This interaction is characterized by the Hamaker constant [39]. This can be calculated by combining the relations method as follows:

$$A_{132} = \left(\sqrt{A_{11}} - \sqrt{A_{33}}\right) \cdot \left(\sqrt{A_{22}} - \sqrt{A_{33}}\right) \tag{5}$$

A_{132} is the Hamaker constant for the DNA–ZnO interaction in a medium of water; it denotes the strength of the interaction.

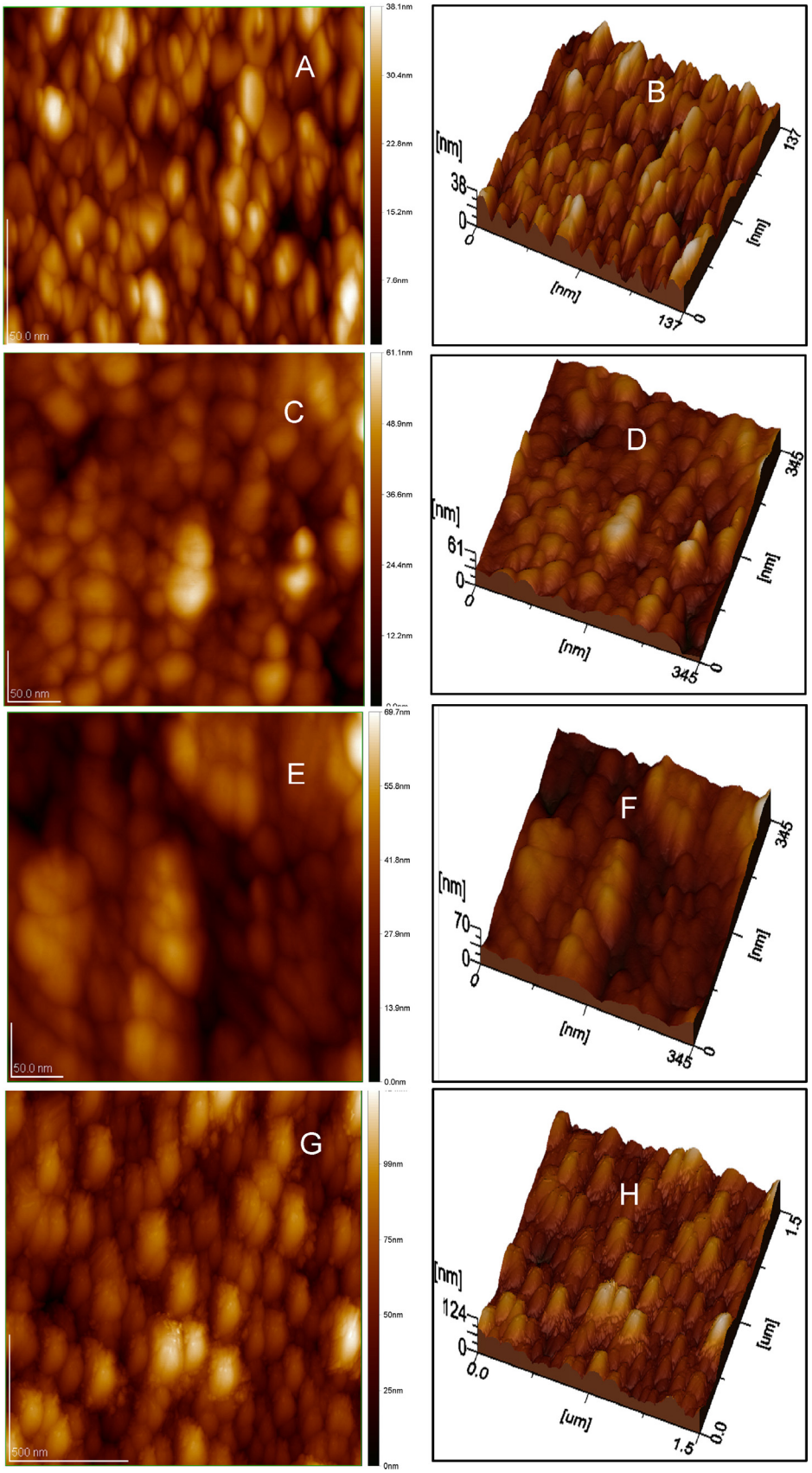

Fig. 7. Atomic force micrographs of the spray-deposited ZnO Thin films. (A) Imaged over the etched edge showing film thickness and (B) surface roughness and porosity.

Applying the known values of A for DNA, water and ZnO, the equation becomes:

$$A_{132} = \left(\sqrt{1.89 \times 10^{-20}} - \sqrt{3.7 \times 10^{-20}}\right) \times \left(\sqrt{0.1 \times 10^{-21}} - \sqrt{3.7 \times 10^{-20}}\right)$$

$$A_{132} = 1.464 \times 10^{-21} \text{ J}$$

This implies that DNA and ZnO interact through electrostatic forces of attraction. This quantifies the van der Waal's forces involved in the system that govern the interaction of the particles. This depends on the properties of the interacting materials and those of the intervening media. The DLVO forces of the interaction comprise 3 principal types of interactions:

- Keesom force: interaction between 2 permanent dipoles.
- Debye forces: interaction between one induced dipole and one permanent dipole.
- London interactions: interaction between 2 induced dipoles.

These interactions are due to the Derjaguin–Landau–Verwey–Overbeek (DLVO) forces present in the solution. According to DLVO theory, the interactions between the particles and their stability can be expressed as a sum of electrostatic and van der Waal's forces. This helps in determining the stability of the particles and is an important factor for the deposition of particles on a rough or porous surface with the transport of particles being mainly controlled by Brownian motion. The interaction between ZnO and DNA in aqueous medium occurs through non-retarded motion. Van der Waals forces are dominant due to the electrical and magnetic polarizations yielding a varying electromagnetic field within the medium as well as in the separation distance between two surfaces [40–42]. Blank ZnO thin film can be used for DNA probe immobilization. Visually, a distinct contrast is observed between the DNA immobilized region and blank region of ZnO thin films. Similarly, where a larger volume of DNA solution was used, the fluorescence becomes more intense. All 4 serotypes of DNA are labelled with respective 5′ labelled fluorescent dye, the details of which are explained in Table 3. Immobilized DNA can be visualized by the addition of an intercalating dye such as SYBR along with the test strand of DNA specific to 4 serotypes. The test strand tends to form loop structures within itself. The intercalating agent intercalates between these strands, resulting in a fluorescent signal when supplied with an excitation during fluorescence scanning. DNA immobilization was confirmed by visualizing the film under fluorescence scanner apparatus.

3.3. Hybridization detection

Rapid differentiation as well as efficacy in identification of the dengue viral serotype is very important as a preventive measure for the spread of disease. For the evaluation of a broad applicability of the ZnO nanoplatform, 2 × 2 array was made to test hybridization detection of the sensing apparatus. Each probe strand was designed in such a way that a fluorescent dye was used for labelling 5′ end of each serotype and then immobilized on ZnO nanoplatform [43]. This modified probe strand is then used for hybridization with a complementary test strand. After DNA hybridization reaction, the fluorescent signal was detected from the duplex DNA using scanning fluorescence measurement. Control experiments were also performed for fluorescence emission detection from as-grown ZnO thin films as well as ZnO thin films immobilized with a 5′ labelled probe strand (data not shown) to confirm the deficiency of any auto-fluorescence. On hybridization with the complementary test strand, fluorescent signals were detected due to the ZnO thin films causing successful fluorescence detection. However, for the detection of as low as 1 nM concentration of fluorophore-labelled DNA molecules using argon laser, SYBR, an intercalating dye, also needs to be used that enhances fluorescent signals that can be determined from Fig. 8. Hence, this work is unique with its capability of using ZnO platforms effectively to differentiate DNA sequence variations of dengue serotype as well as using SYBR as an intercalating agent for enhanced fluorescent detection even at ultratrace levels. It has been observed that metal enhanced fluorescence is responsible for alteration in photonic mode density, thus consequently leading to changes in radiative decay rate. The fluorophores used in our experiment have the disadvantage of having self-quenching property, which is caused by the presence of traps in their energy levels. In

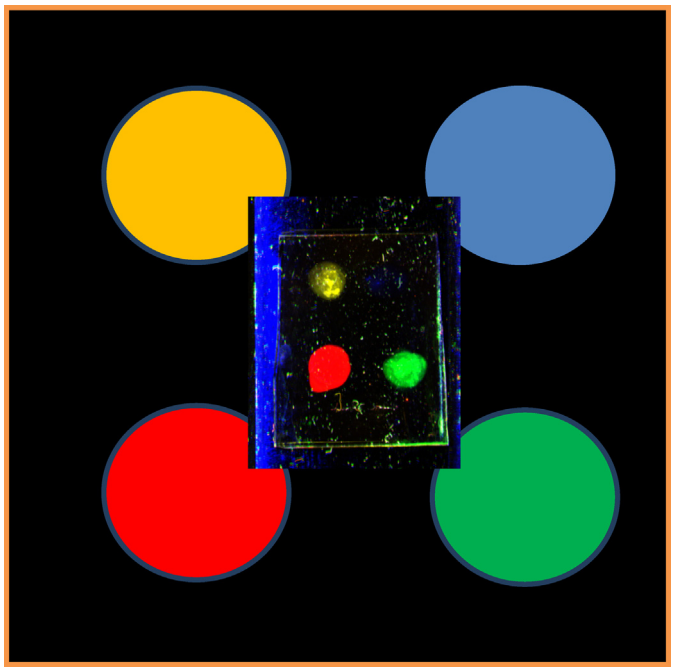

Fig. 8. Simultaneous detection of 4 dengue serotypes (fluorescence scan of hybridization test—inset).

Table 3
Different probe and test strands of 4 different serotypes of dengue. All probe strands are 5′ labelled with their respective fluorescent dyes.

Serotype	Dye (5′ end)	Probe	Test
DENV-1	TEXASRED-6 Camino	5′-GTTTCTTTTCCTAAACACCTCG-3′	5′-CGAGGTGTTTAGGAAAAGAAAC-3′
DENV-2	6-FAM	5′-CCGGTGTGCTCTGCTCTGAT-3′	5′-ATCAGAGCAGAGCACACCGG -3′
DENV-3	Cy5	5′-TTAGAGTTCTTAAGCGTCTCTTG-3’	5′-CAAGAGACGCTTAAGAACTCTAA-3′
DENV-4	YAKIMA YELLOW	5′- CCTGGTTGATGACAAAAGTCTTG-3′	5′-CAAGACTTTTGTCATCAACCAGG-3′

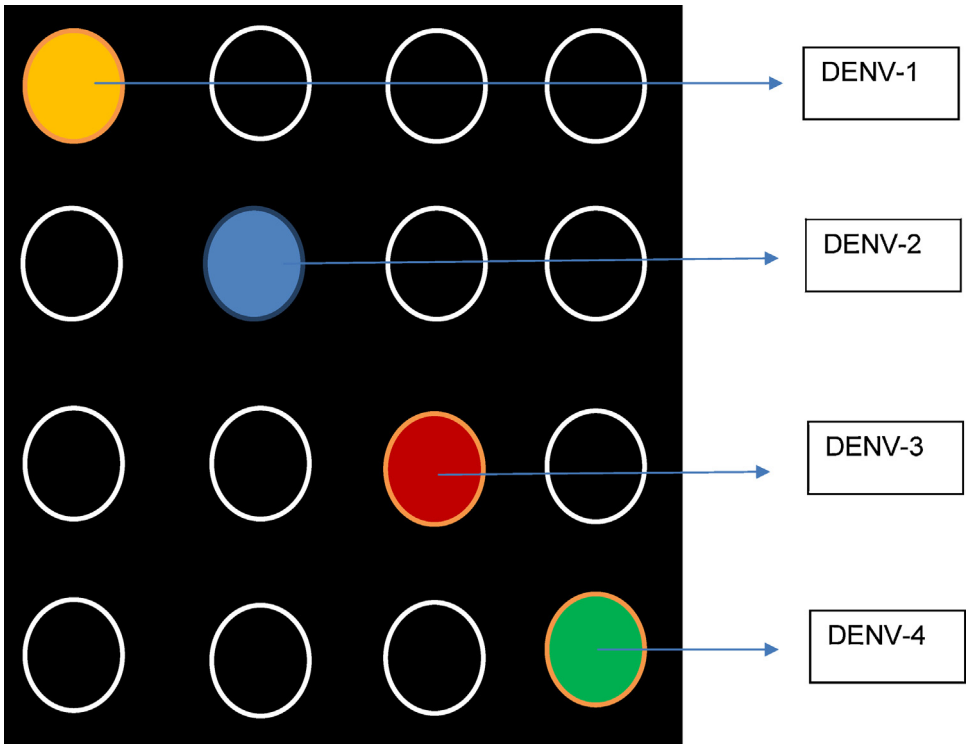

Fig. 9. Simultaneous detection of dengue viral DNA in an array.

this work, we have not only used a ZnO nanoplatform, but also SYBR for disabling such traps and to reduce self-quenching reaction, thus enhancing fluorescence.

In Fig. 8, the signals for all dengue serotypic DNA, DENV-1, DENV-2, DENV-3 and DENV-4 are enhanced using SYBR after the hybridization reaction between the probe and test strands. A 4×4 array was also made as shown in Table 2 and Fig. 9 with *P* representing the probe strand and *T* representing the test strand; subscripts are given to denote the serotype of the virus.

DNA hybridization detection was carried out with *P* and *T* strands both of which have a low concentration of 1 nM, which is significantly less than the conventional concentrations in the range of 1 μM [44], which have been reported while using electrochemical means of detection. This means fewer DNA strands are required for successful detection, and therefore less than 20 μL required for use in micropatterned sensor arrays for the detection of hybridization [45]. However, the method of sensing is similar, being detected by fluorescence signals of a dye. ZnO thin films and SYBR are used for dengue serotypic detection for the following reasons:

1) ZnO substrates are considered to be most reliable, wide band gap transparent metal oxide which can allow fluorescence detection of DNA at lower concentrations.
2) The fluorescent tags on the *P* strands are not uniform in their fluorescence intensity, which warrants the need to use SYBR Green. SYBR Green shows a strong fluorescence and intercalates between the base pairings in the DNA duplex when complementary strands interact. This results in detection of the DNA duplex when the substrate is scanned by the laser scanner equipment.
3) The antireflective nature [46] of the ZnO film enhances the fluorescence of the fluorescent labels and minimizes the scattering of the glass when the laser is directed towards the substrate.

In this article, we have demonstrated for the first time, USP deposited ZnO thin films for dengue serotypic fluorescence detection using DNA as a detection biomolecule. Such fabrication of ZnO thin films is found to be less expensive, less time-consuming and can be conveniently assembled into an array, thus promoting biosensor applications by efficiently coupling conventional apparatus and computerized detection equipment. The transformation and/or integration of ZnO thin films along with DNA as a biomolecule greatly encourage multiplexing and efficient optical sensor arrays.

4. Conclusion

This is for the first time USP deposited thin films with different thicknesses have been engineered to design a fluorescence detection apparatus using dengue viral serotypic DNA. ZnO thin film in comparison to other known substrates is responsible for rapid differentiation of individual DNA serotypes. Such ZnO nanoplatforms can be extraordinarily useful in the accomplishment of specific serotypic detection, particularly with a nanomolar concentration of DNA.

Acknowledgements

The authors would like to thank CINVESTAV-IPN for providing the infrastructural facilities for the completion of this work. The authors would also like to thank Gerardo Perez Ramirez for their expert experimental help. We also acknowledge CINVESTAV authorities for the funds provided through the joint project between CINVESTAV and the University of Cranfield.

References

[1] S.B. Halstead, Pathogenesis of dengue: challenges to molecular biology, Science 239 (4839) (1988) 476–481.
[2] M.G. Guzman, S.B. Halstead, H. Artsob, P. Buchy, J. Farrar, D.J. Gubler, E. Hunsperger, A. Kroeger, H.S. Margolis, E. Martínez, M.B. Nathan, J.L. Pelegrino, C. Simmons, S. Yoksan, R.W. Peeling, UNICEF/UNDP/World Bank/WHO Special Programme for Research and Training in Tropical Diseases (TDR), World Health Organization Geneva, Switzerland, 2010.

[3] B.L. Innis, A. Nisalak, S. Nimmannitya, S. Kusalerdchariya, V. Chongswasdi, S. Suntayaborn, P. Puttisri, C.H. Hoke, An enzyme-linked immunosorbent assay to characterize dengue infections where dengue and Japanese encephalitis co-circulate, Am. J. Trop. Med. Hyg. 40 (4) (1989) 418–427.
[4] D.H. Clarke, J. Casals, Techniques for hemagglutination and hemagglutination-inhibition with arthropod-borne viruses, Am. J. Trop. Med. Hyg. 7 (1958) 561–573.
[5] S. Vene, J. Mangiafico, B. Nicklasson, Clinical and diagnostic virology indirect immunofluorescence for serological diagnosis of dengue virus infections in Swedish patients, Clin. Diagn. Virol. 4 (1995) 43–50.
[6] K.R. Porter, S. Widjaja, H.D. Lohita, S.H. Hadiwijaya, C.N. Maroef, W. Suharyono, R. Tan, Evaluation of a commercially available immunoglobulin M capture enzyme-linked immunosorbent assay kit for diagnosing acute dengue infections, Clin. Diagn. Lab. Immunol. 6 (1999) 741–744.
[7] P.R. Young, P.A. Hilditch, C. Bletchly, W. Halloran, An antigen capture enzyme-linked immunosorbent assay reveals high levels of the dengue virus protein NS1 in the sera of infected patients an antigen capture enzyme-linked immunosorbent assay reveals high levels of the dengue virus protein NS1 in the sera, J. Clin. Microbiol. 38 (2000) 1053–1057.
[8] P.K. Russell, A. Nisalak, Dengue virus identification by the plaque reduction neutralization test, J. Immunol. 99 (1967) 291–296.
[9] M. Zimmer, Green fluorescent protein (GFP): applications, structure, and related photophysical behavior, Chem. Rev. 102 (3) (2002) 759–781.
[10] T.A. Taton, C.A. Mirkin, R.L. Letsinger, Scanometric DNA array detection with nanoparticle probes, Science 289 (5485) (2000) 1757–1760.
[11] A.D. McFarland, R.P. Van Duyne, Single silver nanoparticles as real-time optical sensors with zeptomole sensitivity, Nano Lett. 3 (8) (2003) 1057–1062.
[12] H. Wu, M. Xue, J. Ou, F. Wang, W. Li, Effect of annealing temperature on surface morphology and work function of ZnO nanorod arrays, J. Alloys Comp. 565 (2013) 85–89.
[13] H. Li, Z. Zhang, J. Huang, R. Liu, Q. Wang, Optical and structural analysis of rare earth and Li co-doped ZnO nanoparticles, J. Alloys Comp. 550 (2013) 526–530.
[14] C. Klingshirm, The luminescence of ZnO under high one- and two-quantum excitation, Phys. Status Solidi B 71 (2) (1975) 547–556.
[15] J.J. Hassan, M.A. Mahdi, Y. Yusof, H. Abu-Hassan, Z. Hassan, H.A. Al-Attar, A.P. Monkman, Fabrication of ZnO nanorod/p-GaN high-brightness UV LED by microwave-assisted chemical bath deposition with $Zn(OH)_2$–PVA nanocomposites as seed layer, Opt. Mater. 35 (5) (2013) 1035–1041.
[16] A.M.K. Dagamseh, B. Vet, F.D. Tichelaar, P. Sutta, M. Zeman, ZnO:Al films prepared by rf magnetron sputtering applied as back reflectors in thin-film silicon solar cells, Thin Solid Films 516 (21) (2008) 7844–7850.
[17] C.S. Rout, A.R. Raju, A. Govindaraj, C.N.R. Rao, Hydrogen sensors based on ZnO nanoparticles, Solid State Commun. 138 (3) (2006) 136–138.
[18] W.I. Park, J.S. Kim, G.C. Yi, M.H. Bae, H.J. Lee, Fabrication and electrical characteristics of high-performance ZnO nanorod field-effect transistors, Appl. Phys. Lett. 85 (21) (2004) 5052–5054.
[19] M. Huang, S. Mao, H. Feick, H. Yan, Y. Wu, H. Kind, E. Weber, R. Russo, P. Yang, Room-temperature ultraviolet nanowire nanolasers, Science 292 (5523) (2001) 1897–1899.
[20] C. Xu, X.W. Sun, Field emission from zinc oxide nanopins, Appl. Phys. Lett. 83 (18) (2003) 3806–3808.
[21] Y. Liu, M. Zhong, G. Shan, Y. Li, B. Huang, G. Yang, Biocompatible ZnO/Au nanocomposites for ultrasensitive DNA detection using resonance Raman scattering, J. Phys. Chem. B 112 (20) (2008) 6484–6489.
[22] K. Yang, G.W. She, H. Wang, X.M. Ou, X.H. Zhang, C.S. Lee, S.T. Lee, ZnO nanotube arrays as biosensors for glucose, J. Phys. Chem. C 113 (47) (2009) 20169–20172.
[23] X. Zhu, I. Yuri, X. Gan, I. Suzuki, G. Li, Electrochemical study of the effect of nano-zinc oxide on microperoxidase and its application to more sensitive hydrogen peroxide biosensor preparation, Biosens. Bioelectron. 22 (8) (2007) 1600–1604.
[24] A. Umar, M.M. Rahman, M. Vaseem, Y.B. Hahn, Ultra-sensitive cholesterol biosensor based on low-temperature grown ZnO nanoparticles, Electrochem. Commun. 11 (1) (2009) 118–121.
[25] Y.F. Li, Z.M. Liu, Y.L. Liu, Y.H. Yang, G.L. Shen, R.Q. Yu, A mediator-free phenol biosensor based on immobilizing tyrosinase to ZnO nanoparticles, Anal. Biochem. 349 (1) (2006) 33–40.
[26] T. Ma, S. Lee, Effects of aluminium content and substrate temperature on the structural and electrical properties of aluminium-doped ZnO films prepared by ultrasonic spray pyrolysis, J. Mater. Sci.: Mater. Electron. 1 (2000) 305–309.
[27] T.R. Ramireddy, V. Venugopal, J.B. Bellam, A. Maldonado, J. Vega-pérez, S. Velumani, M.D.L.L. Olvera, Effect of the milling time of the precursors on the physical properties of sprayed aluminum-doped zinc oxide (ZnO:Al) thin films, Materials (Basel) 5 (12) (2012) 1404–1412.
[28] R. Biswal, L. Castañeda, R. Moctezuma, J. Vega-Pérez, M.D.L.L. Olvera, A. Maldonado, Formation of indium-doped zinc oxide thin films using ultrasonic spray pyrolysis: the importance of the water content in the aerosol solution and the substrate, Materials (Basel) 5 (12) (2012) 432–442.
[29] D.F. Paraguay, L.W. Estrada, D.R. Acosta, M.E. Andrade, M. Yoshida, Growth, structure and optical characterization of high quality ZnO thin films obtained by spray pyrolysis, Thin Solid Films 350 (2) (1999) 192–202.
[30] J.A. Dirksen, T.A. Ring, Fundamentals of crystallization: kinetic effects on particle size distributions and morphology, Chem. Eng. Sci. 46 (10) (1991) 2389–2427.
[31] Y.S. Kim, W.P. Tai, S.J. Shu, Effect of preheating temperature on structural and optical properties of ZnO thin films by sol–gel process, Thin Solid Films 491 (1–2) (2005) 153–160.
[32] I. Akyuz, S. Kose, F. Atay, V. Bilgin, The optical, structural and morphological properties of ultrasonically sprayed ZnO:Mn films, Semicond. Sci. Technol. 21 (12) (2006) 1620–1626.
[33] J. Tauc, Amorphous and Liquid Semiconductor, Plenum, London, 1974.
[34] N.F. Mott, E.A. Davis, Electronic Processes in Non-Crystalline Materials, Oxford, Clarendon, 1979.
[35] R.E. Marotti, D.N. Guerra, C. Bello, G. Machado, E.A. Dalchiele, Bandgap energy tuning of electrochemically grown ZnO thin films by thickness and electrodeposition potential, Solar Energy Mater. Solar Cells 82 (1–2) (2004) 85–103.
[36] B.D. Cullity, Elements of X-Ray Diffraction, Addison-Wesley, MA, 1978.
[37] A. Degen, M. Kosec, Effect of pH and impurities on the surface charge of zinc oxide in aqueous solution, J. European Ceramic Soc. 20 (2000) 667–673.
[38] M. Das, G. Sumana, R. Nagarajan, B.D. Malhotra, Application of nanostructured ZnO films for electrochemical DNA biosensor, Thin Solid Films 519 (3) (2010) 1196–1201.
[39] G. Lefevre, A. Jolivet, Calculation of Hamaker constants applied to the deposition of metallic oxide particles at high temperature, in: Proceedings of International Conference on Heat Exchanger Fouling and Cleaning, 2009, pp. 120–124, Vol. VIII.
[40] L. Bergström, Hamaker constants of inorganic materials, Adv. Colloid Interface Sci. 70 (1997) 125–169.
[41] S. Thennadil, L. Garcia-Rubio, Approximations for calculating van der Waals interaction energy between spherical particles—a comparison, J. Colloid Interface Sci. 243 (2001) 136–142.
[42] M. Singh-Zocchi, S. Dixit, V. Ivanov, G. Zocchi, Single-molecule detection of DNA hybridization, Proc. Natl Acad. Sci. 100 (13) (2003) 7605–7610.
[43] A. Dorfman, N. Kumar, J. Hahm, Highly sensitive biomolecular fluorescence detection using nanoscale ZnO platforms, Langmuir 22 (11) (2006) 4890–4895.
[44] W. Zhang, T. Yang, D. Huang, K. Jiao, G. Li, Synergistic effects of nano-ZnO/multi-walled carbon nanotubes/chitosan nanocomposite membrane for the sensitive detection of sequence-specific of PAT gene and PCR amplification of NOS gene, J. Memb. Sci. 325 (1) (2008) 245–251.
[45] N. Kumar, A. Dorfman, J. Hahm, Ultrasensitive DNA sequence detection using nanoscale ZnO sensor arrays, J. Nanotechnol. 17 (12) (2006) 2875–2881.
[46] S. Sali, M. Boumaour, M. Kechouane, S. Kermadi, F. Aitamar, Nanocrystalline ZnO film deposited by ultrasonic spray on textured silicon substrate as an anti-reflection coating layer, Phys. B: Condens. Matter 407 (13) (2012) 2626–2631.

Biographies

M. Adiraj Iyer received his MTech degree (2013) in medical nanotechnology from SASTRA University, Thanjavur, India. He was a visiting student at CINVESTAV-IPN, Mexico during Jan-Jun 2013 through the semester abroad programme of SASTRA University. His research interest includes thin films, biomaterials, tissue engineering, bioengineering and medical nanotechnology.

Goldie Oza has done MSc in life sciences (specialization in biotechnology) and PhD in botany in the year 2003 and 2012, respectively. After his PhD on the topic of Biosynthesis of Nanometals and its application in cancer and alzheimer's disease, he joined as a postdoctoral fellow in CINVESTAV, Mexico D.F. on synthesis of metal nanoparticles and their applications in Biosensing, Hyperthermia, photothermal therapy, and drug-delivery. He is specialized in chemical and biological synthesis of zinc oxide, titanium oxide, quantum dots, SPIONs, carbon nanotubes and graphene quantum dots. He has written a book, Bionanotechnology: concepts and its applications, published by CRC press. He has 36 publications in peer-reviewed journals, to his credit.

S. Velumani received MSc degree in Physics and PhD in Thin Film Physics from Bharathiar University in the year 1985 and 1998 respectively. He was employed as lecturer/assistant professor in the department of Physics, Coimbatore Institute of Technology for 15 years. He also worked as a researcher in Solar-Hydrogen Fuel cell group in UNAM, Temixco in Mexico and Mexican Petroleum Research center from 2001 to 2005. Later he joined as research professor and co-ordinator in the materials science group of Physics department in ITESM, Monterey, Mexico. From 2008, he is a full time professor in the Electronics and Solid State Section of Electrical Engineering Department at CINVESTAV-IPN, Mexico. His research interest includes synthesis and characterization of CIGS, CZTS, ZnO, carbon nanotubes, graphene for solar cell applications. He is also a connoisseur in synthesis of $BiVO_4$, TiO_2, SPIONS and core-shell (Au-Fe_3O_4) nanoparticles for photocatalytic and biomedical applications. He has published more than 80 research articles in peer-reviewed international journals and has more than 600 citations. He was also guest editor for about 10 special issues from publishers like Elsevier, Springer, TransTech etc.

Arturo Maldonado has obtained his bachelors' degree in Mathematical Physics and then received his Ph.D. in the year 1997 in department of Electrical Engineering, CINVESTAV; Mexico D.F. He is a distinguished scientist and has teaching experience of almost 29 years. His research interest includes zinc oxide thin films, coatings, sensors and is specialized in various methods such as Spray Pyrolysis, sol-gel etc.

Josue Romero received his bachelor's degree in Physics and masters in Materials Sciences in the year 2009 and 2011 respectively, from National Autonomous University of Mexico (UNAM). He has lectured in more than 25 international and national conferences and has 5 publications having high impact factor. He has a teaching experience at the undergraduate level in physics for over 7 years (UNAM). He has developed and participated in national and international projects. He is currently

working in electron microscopy at the Advanced Electronics Laboratory Nanoscopy (LANE) and is responsible for FESEM and SPM.

M. Sridharan received his MSc - Physics (University of Madras) in 1997 and PhD – Physics - Thin Film Science & Technology (Bharathiar University) in 2003. During his doctoral studies he worked as a visiting research student at Korea Advanced Institute of Science and Technology (KAIST), Republic of Korea (2001). He worked as a postdoctoral researcher at Universitat Autonoma de Barcelona (UAB), Spain (2003-2004) and Inha University, Republic of Korea (Jan-Nov 2005). He also worked as an assistant professor/postdoctoral Researcher at the Interdisciplinary Nanoscience Center (iNANO), University of Aarhus, Denmark (Dec. 2005 - May 2008). Currently he is at the Functional Nanomaterials & Devices Lab, Centre for Nanotechnology & Advanced Biomaterials (CeNTAB) and School of Electrical & Electronics Engineering, SASTRA University, India. His research interest includes thin films, coatings, sensors, solar cells, hydrogen energy, biomaterials, MEMS and functional nanomaterials & devices.

M. De L. Muñoz received bachelor's degree in Biochemical Engineering from National School of Biological Sciences from the National Polytechnic Institute (IPN). She obtained MSc and PhD degree at the Center for Research and Advanced Studies of IPN (CINVESTAV-IPN) in Mexico City. She obtained a postdoctoral fellowship award from the National Institute of Allergy and Infectious diseases in USA and she is research professor in the Department of Genetics and Molecular Biology at CINVESTAV-IPN since 1985. The research in her laboratory spans several topics in genetics, with focus in detecting serotype and genotype of Dengue virus based on DNA microarray assay. Her research also includes genetic studies on the dengue transmitter Aedes aegypti mosquito, and human genetics of prehispanic and contemporary mexican populations. In addition she is studying dengue receptors in epithelial cells of mosquitoes of A. aegypti. She has published multiple research papers and book chapters (more than 100). Furthermore, she has one international patent.

R. Asomoza is presently Director General of the Center for Research and Advanced Studies of IPN (CINVESTAV). He graduated at the School of Physics and Mathematics of National Polytechnic Institute, Puebla, Mexico in 1972. He obtained his doctorate in Solid State Physics from the University of Paris XI, Orsay, France 1975 under the guidance of Prof. Albert Fert, Nobel Prize winner for Physics in 2007. He joined CINVESTAV as research professor "D" in department of electrical engineering in 1980. He has served as head of the electrical engineering Department (1996–1999), Provost (1999–2003) of Cinvestav. His main research areas are magnetic and electrical properties of rare earths in different metallic matrices, managing to elucidate the contribution of magnetic order in the transport properties of amorphous alloys. Recently his field of interest is surface properties of semiconductors and devices by the technique of mass spectrometry, secondary ion. He has published 113 research papers in journals of international circulation, 32 publications in international conference proceedings, 17 national events, three technical reports, articles and 6 reviews.

Junsin Yi received the PhD degree in Electrical Engineering from State University of New York at Buffalo, USA in 1994. He became a professor in the department of Electrical Engineering at the Sungkyunkwan University (SKKU) in 1995. Currently, he is Director of the Interdisciplinary graduate school program for Photovoltaic specialist (IPPs) in SKKU. Starting from 2006, Korean Government Ministry of Knowledge and Economy supported IPPs program in SKKU to meet the need of human resource in PV industry. He has contributed to Korean National Plans for the renewable energy sources as a Korea Presidential Advisory Board member in 2007. He was the first person to initiate industry oriented silicon solar cell R&D and to proof solar cell mass production is possible in Korea. From 2001 to 2007, he served as CEO and Head of R&D KPE Solar Cell Company in Korea. From 2009, he has been nominated as a Fellow professor in SKKU. He has successfully guided more than seventy students for PhD and MS degrees as their advisor over 16 years in SKKU. He has published 4 solar cell text books for the industrial new comers, undergraduate level students, and R&D oriented research engineer. He has more than 150 international publications in SCI listed journals and contributed more than 300 papers in the proceedings of international conferences/symposia. His research areas are crystalline silicon solar cells, Hetero-junction with Intrinsic Thin film (HIT) solar cells, amorphous silicon thin film solar cells, and nano or micro silicon thin film solar cells.